On the Origin and Spread of an Adaptive Allele in Deer Mice

Catherine R. Linnen,[1]* Evan P. Kingsley,[1] Jeffrey D. Jensen,[2] Hopi E. Hoekstra[1]

Adaptation is a central focus of biology, although it can be difficult to identify both the strength and agent of selection and the underlying molecular mechanisms causing change. We studied cryptically colored deer mice living on the Nebraska Sand Hills and show that their light coloration stems from a novel banding pattern on individual hairs produced by an increase in *Agouti* expression caused by a *cis*-acting mutation (or mutations), which either is or is closely linked to a single amino acid deletion in *Agouti* that appears to be under selection. Furthermore, our data suggest that this derived *Agouti* allele arose de novo after the formation of the Sand Hills. These findings reveal one means by which genetic, developmental, and evolutionary mechanisms can drive rapid adaptation under ecological pressure.

To unravel evolutionary mechanisms in the wild, we must estimate the fitness advantage of adaptive alleles and infer their source, either as new or preexisting variation. In the Sand Hills of Nebraska, deer mice (*Peromyscus maniculatus*) have evolved a dorsal coat that closely matches their local habitat (Fig. 1A and fig. S1). The Sand Hills are a dune field with soil mostly consisting of quartz grains (*1*, *2*) that are lighter in color than the surrounding soils. *P. maniculatus* coat color is correlated with this soil color (*3*), which is probably due to selection against avian predation (*4*). Because light-colored mice are conspicuous prey on dark soils (*5*) and because the Sand Hills are geologically young [dating between the end of the Wisconsin glacial period (10,000 to 15,000 years ago) to within the last 8000 years (*6*, *7*)], the light coat coloration in Sand Hills mice represents a recent adaptation.

Wider hair bands make lighter mice. To a large extent, variation in mammalian pigmentation can be explained by the distribution and relative amounts of brown-black eumelanin and yellow-red pheomelanin pigments in individual hairs (*8*, *9*). Pigment-producing cells (melanocytes) at the base of hair follicles can switch between the production of these pigments during hair growth, resulting in hairs with different banding patterns. Many mammals, including laboratory mice, can have hairs containing a subapical band of pheomelanin on an otherwise eumelanic hair. In *Peromyscus*, this pheomelanic band is markedly wider in Sand Hills mice than in their darker conspecifics (Fig. 1B). Accordingly, the light Sand Hills phenotype has been dubbed "wideband" (*10*).

To evaluate the relationship between a mouse's overall lightness and the size of pheomelanic bands on its dorsal hairs, we compared band width and brightness in five wideband and five wild-type *P. maniculatus* (Fig. 1C). Band width was measured by excising skin plugs from the dorsum and measuring the relative areas of yellow and black pigments in micrographs of the attached hairs (Fig. 1B) (*11*). We quantified pelt brightness by measuring the percentage of light reflected using a spectrophotometer and found that band width and reflectance were strongly correlated ($R^2 = 0.849$; analysis of variance; $n =$ 10 mice, $P = 0.00015$) (Fig. 1C). Thus, the increased width of the subapical pheomelanic band on dorsal hairs is, to a large degree, responsible for the overall lighter color in mice derived from the Sand Hills.

***Agouti* is responsible for the wideband phenotype.** Given its role in producing pheomelanin and its known phenotypic effects, *Agouti* is a strong candidate for the gene causing the wideband phenotype. In *Mus musculus*, knockouts of *Agouti* result in eumelanic (dark-colored) mice, overexpression of *Agouti* results in pheomelanic (light-colored) mice, and light alleles are generally dominant to dark ones (*12*–*14*). Consistent with this dominance hierarchy, we found that all offspring from a cross between pure wideband (a^{wb}/a^{wb}) and pure wild-type (a^{+}/a^{+}) *P. maniculatus* were phenotypically wideband ($n = 31$ mice). Furthermore, a pulse of *Agouti* expression during hair growth in wild-type *M. musculus* correlates with the production of subapical pheomelanic bands (*12*, *15*). To determine whether the wideband phenotype in *Peromyscus* is caused by *Agouti*, we intercrossed *P. maniculatus* that were heterozygous for nonagouti (a^{-}) (*16*), which is a melanic strain resulting from a recessive 125-kb deletion lacking *Agouti* expression (*17*). The resulting ratio of wideband: nonagouti phenotypes among the offspring did not differ significantly from 3:1 (χ^2 test; $n = 49$ mice, $P = 0.46$) (table S1), suggesting that the wideband phenotype segregates as a single dominant *Agouti* allele (*18*). Furthermore, the 125-kb deletion segregated perfectly with coat-color phenotype among the offspring; markers for other pigmentation genes (*attractin* and *tyrosinase-related protein 1*) did not (table S1). Finally, no sequence differences were observed between wild-type, wideband, and nonagouti *P. maniculatus* in the *melanocortin-1 receptor* (*Mc1r*)–coding region ($n = 7$ a^{wb}/a^{-}; $n = 2$ a^{-}/a^{-}, and $n = 1$ a^{+}/a^{+}, respectively).

Agouti mRNA levels in wideband/nonagouti *P. maniculatus* were significantly higher than in wild-type/nonagouti mice (a^{wb}/a^{-} versus a^{+}/a^{-} *t* test, $n = 8$ mice, $P = 0.0069$, one-tailed) (Fig. 2A). This expression difference persisted when abundance of both alleles was measured separately in a^{wb}/a^{+} heterozygotes (a^{wb} versus a^{+} *t* test; $n = 8$ alleles, $P = 0.00031$, one-tailed) (Fig. 2A), demonstrating that one or more mutations acting in *cis* lead to an increase in *Agouti* expression (*19*). These data indicate that a *cis*-acting mutation (or mutations) in, or linked to, the *Agouti* gene is responsible for the wideband phenotype.

We also measured *Agouti* mRNA levels over a synchronized hair cycle (as hairs first emerge simultaneously in newborn mice) in neonatal wideband and wild-type *P. maniculatus*. Because *Agouti* initiates the production of the pheomelanic hair band during a pulse of expression occurring postnatally from day 3 to 7 in *Mus musculus* (*15*), we measured *Agouti* expression between birth and day 8 in wideband and wild-type *P. maniculatus* (Fig. 2B). Between days 1 and 5 inclusively, *Agouti* mRNA was significantly more abundant in wideband mice than in wild-type (*t* tests; $n = 7$ to 9 mice for each time point, $P < 0.05$, one-tailed) (Fig. 2B). Although *Agouti* expression peaks at day 4 in both wideband and wild-type mice, in wideband mice expression peaks above wild-type levels by day 1 and remains at or above this level until day 7 (Fig. 2B). Thus, the pulse of *Agouti* expression during hair growth is both longer and higher in wideband postnatal mice, suggesting that increased *Agouti* expression is the underlying cause of the wideband phenotype in *P. maniculatus*.

Agouti produces two transcriptional isoforms, each with a different expression profile (*15*, *20*). The hair cycle–specific isoform that produces the hair band in *Mus* contains untranslated exons 1B or 1C and is expressed in a timed pulse during hair growth (*15*). We sequenced exons 1B, 1C, 2, 3, and 4 in four wideband and four wild-type *P. maniculatus* and compared these with a *P. maniculatus rufinus* individual with a wild-type phenotype, as an outgroup. Within the transcript expressed in the hair cycle, we identified 20 nucleotide differences between wideband and wild-type mice, 11 of which were derived relative to the outgroup in wideband mice (Fig. 3A). Seven

[1]Department of Organismic and Evolutionary Biology and the Museum of Comparative Zoology, Harvard University, 26 Oxford Street, Cambridge, MA 02138, USA. [2]Center for Theoretical Evolutionary Genomics, Department of Integrative Biology, University of California, Berkeley, 3060 Valley Life Sciences Building, Berkeley, CA 94720, USA.

*To whom correspondence should be addressed. E-mail: clinnen@oeb.harvard.edu

differences (four derived) were observed within the coding region, of which two resulted in amino acid changes in wideband mice, a conservative amino acid substitution (Arg37Lys) and a serine deletion (residue 48), both in exon 2. All polymorphisms were perfectly associated with the wideband phenotype in laboratory populations of *Peromyscus*.

Wideband allele frequency in natural populations. To test whether any of these *Agouti* polymorphisms were associated with the wideband phenotype in nature, we captured 91 individuals from two phenotypically variable populations near the edge of the Sand Hills (Fig. 1A and table S2). We collected phenotypic (band width and brightness) and genotypic (*Agouti* hair-cycle transcript sequence and alleles at seven microsatellite markers) data for each individual. We pooled individuals from the two locations for association tests because we did not detect differences in color among the populations (brightness, *t* test; $n = 91$ mice, $P = 0.90$, two-tailed). Moreover, although the program STRUCTURE (*21*, *22*) identified two genetic clusters ($K = 2$), which corresponded to geography [Fisher's exact test; $n = 85$ mice, $P = 0.0039$; mean fixation index (F_{ST}) across seven microsatellite loci was 0.020 ± 0.003 SEM], there was no correlation with phenotype (brightness, *t* test; $n = 91$ mice, $P = 0.89$, two-tailed). These results suggest that mice do not mate assortatively on the basis of coat color and that dark-colored mice are not recent, genetically distinct migrants. Therefore, we hypothesized that light and dark mice interbreed with ample opportunity for recombination between the wideband and wild-type alleles.

Because band width and brightness were more variable in Sand Hills mice than in the laboratory populations (fig. S2, A and B), we used quantitative measures of both band width and brightness, rather than discrete categories, for association tests. At the *Agouti* locus, most of the hair-cycle transcript polymorphisms identified in the lab were also variable among Sand Hills mice (Fig. 3A). Of these candidate polymorphisms, only the serine deletion in exon 2 explained variation in band width (13.2% of the observed variation) and in overall brightness (8.8% of variation) after correction for multiple comparisons (Fig. 3A) and was consistent with observed dominance patterns from laboratory crosses. Specifically, individuals with one or more copies of the deletion ($a^{\Delta Ser/-}$) were significantly lighter than those without (a^{+}/a^{+}) (*t* tests; $n = 91$ mice; band width, $P = 0.00020$, one-tailed; brightness, $P = 0.0022$, one-tailed), whereas heterozygotes ($a^{\Delta Ser}/a^{+}$) and homozygotes ($a^{\Delta Ser}/a^{\Delta Ser}$) were phenotypically indistinguishable (*t* tests; $n = 62$ mice; band width, $P = 0.81$, two-tailed; brightness, $P = 0.39$, two-tailed).

This serine deletion occurs in an evolutionarily conserved region of the Agouti protein that interacts with Attractin, an accessory receptor thought to facilitate Agouti's role in pigment-switching (*23*). It is therefore possible that the serine deletion is directly responsible for the wideband phenotype. Alternatively, the deletion could be in linkage disequilibrium (LD) with the causal mutation (or mutations). We thus examined pat-

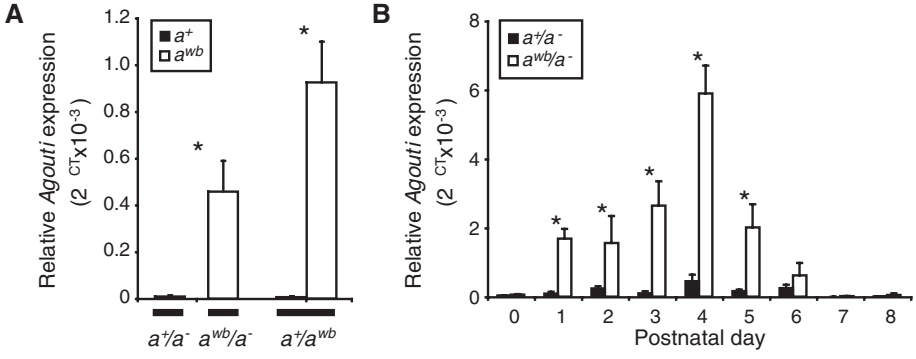

Fig. 2. A *cis*-acting mutation (or mutations) increases *Agouti* expression and causes the wideband phenotype. (**A**) Quantitative real-time polymerase chain reaction assays show that *P. maniculatus* with the wideband allele (a^{wb}) express *Agouti* at a higher level than do those with the wild-type allele (a^{+}). In heterozygotes (a^{+}/a^{wb}), the a^{wb} allele is expressed at a higher level than the a^{+} allele, suggesting that the causal mutation (or mutations) acts in *cis*. (**B**) Expression of *Agouti* transcript is significantly higher in wideband mice from postnatal day 1 to day 5 (asterisks denote significance at $P < 0.05$, *t* test, $n = 3$ to 6 mice for each genotype and time point). *Agouti* expression was measured relative to β-actin; data are mean ± SEM.

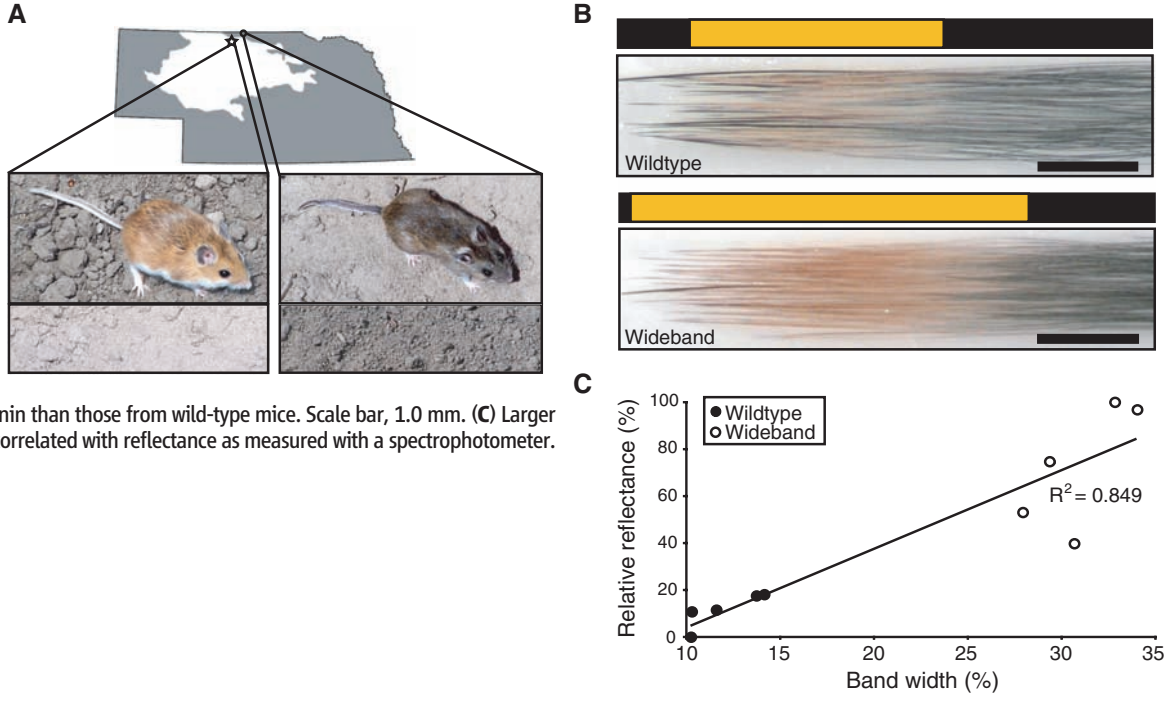

Fig. 1. Soil and mice are brighter on the Sand Hills because of band width. (**A**) Approximate location of Sand Hills within Nebraska. Typical soil (bottom) and mouse (top) colors for populations sampled on (star) and off (circle) the Sand Hills. Mice are shown on contrasting soil backgrounds. (**B**) Hairs from the dorsum of wideband mice have a wider band of pheomelanin than those from wild-type mice. Scale bar, 1.0 mm. (**C**) Larger band area is significantly correlated with reflectance as measured with a spectrophotometer.

terns of LD upstream and downstream of the deletion. We observed significant LD across the entire 1-kb region flanking exon 2 and found that LD rapidly decays downstream (3′), but not upstream (5′), of the deletion (Fig. 3B) when we examined high-frequency polymorphisms (the minor allele frequency was >10%). Additionally, LD persisted as far as 19 kb upstream of the deletion but not past 600 bp downstream (table S3). On the basis of these results, we cannot determine whether the serine deletion, a linked mutation, or both cause wide bands and light coats. Given the rapid decay of LD downstream of the deletion, the observed extended upstream LD may be due to epistatic selection on multiple coadapted mutations (*24*, *25*). Nonetheless, the haplotype containing the serine deletion (hereafter "wideband haplotype" or "wideband allele") explains a substantial amount of ecologically relevant phenotypic variation.

Selection on the wideband haplotype. To compare putatively adaptive (wideband or $a^{\Delta Ser}$) and neutral (wild-type or a^{+}) haplotypes, we examined nucleotide variation in the two haplotype classes. A significant reduction in variation, which was consistent with patterns expected under a selective sweep, was observed in the wideband haplotype as compared with that in the wild-type haplotype [number of segregating sites (S) = 52 and nucleotide diversity (π) = 0.0081 for n = 80 wideband versus S = 80 and π = 0.0133 for n = 102 wild type] (Fig. 4A). We also found that the shape of the full site frequency spectra (SFS) for the haplotype classes differed between wild-type and wideband haplotypes (fig. S3). The wild-type haplotype was not distinguishable from that predicted under a neutral equilibrium model, whereas the wideband haplotype showed a strong skew in the SFS, matching a hitchhiking model (a U-shaped SFS).

To distinguish between selective and neutral models, we performed a composite likelihood ratio (CLR) test (*26*) and separately evaluated the evidence for selection on the wideband and wild-type haplotypes [following the method in (*27*)]. A significant signature of positive selection was observed for the wideband haplotype (CLR test; P = 0.012) but not on the remaining chromosomes (CLR test; P = 0.123). We then used the goodness-of-fit (GOF) test (*28*) on the wideband haplotype and found that the hitchhiking model could not be rejected (GOF P = 0.813). Finally, we employed the ω_{max} statistic (*29*, *30*) and found that the LD patterns across the wideband haplotype were significantly different from those expected under neutrality (ω_{max}; P = 0.041), whereas LD patterns for the wild-type haplotype classes were not (ω_{max}; P = 0.345). Together, these results demonstrate that selection is probably acting on the wideband *Agouti* haplotype.

Additionally, these analyses identified a location at or near the serine deletion that is the nucleotide site that maximizes the significance of the CLR and ω test statistics (*26*, *29*) and thus is the most likely target of selection in our data (Fig. 3B). Because patterns of variation around a selected site may only be expected to be symmetric on average, but not in any individual realization (*26*), the noted patterns of asymmetric LD surrounding the deletion are consistent with our conclusion (Fig. 3B).

Strength and timing of selection. To estimate the selection coefficient acting on the wideband haplotype, we obtained maximum likelihood estimates of $\alpha = 2Ns$, where N is the effective population size, via maximization of the composite likelihood function (*26*) and found an estimate of α = 112. Assuming N = 10,000 (*31*), this corresponds to an estimated selection coefficient of s = 0.0056. Using a parametric bootstrap (*32*), we obtained a 95% confidence interval (CI) (constructed with the percentile method) that spans from α = 56 to α = 207 (s = 0.0028 to 0.0104). Based on owl predation experiments (*4*) and the observed *Agouti* allele frequencies, we estimated that when on light soil wideband mice have a selective advantage s = 0.102 as compared with darker mice. This is certainly an overestimate of selection, given that predation rates were most likely artificially inflated in the enclosed arena tested (*4*) and that other loci probably contribute to the Sand Hills mouse phenotype. Nevertheless, both population genetic data and predation experiments suggest that selection for light color is strong, and our estimates fall within the range of selection coefficients for other color polymorphisms, including in beach mice (*33*), pocket mice (*5*), ladybirds (*34*), and land snails (*35*).

Based on our estimates of the selection strength acting on the wideband allele, we inferred the timing of selection on this allele. From

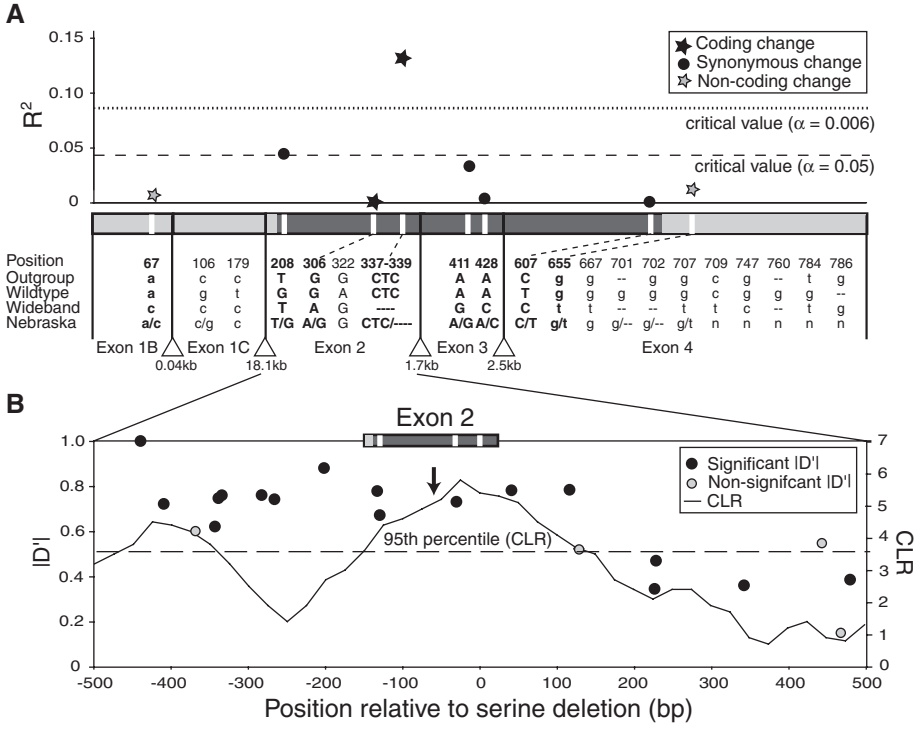

Fig. 3. A coding deletion in exon 2 is associated with band width and sweeplike patterns of genetic variation. (**A**) The correlation (R^2) between genotype and phenotype (band width) in a natural population. Hair-cycle transcript exons (*x* axis) are drawn to scale and coded as follows: translated regions are in dark gray and uppercase; untranslated regions are in light gray and lowercase; and introns are indicated by triangles. Significance thresholds are before (α = 0.05) and after (α = 0.006) Bonferroni correction. Listed are all sites that differed between wideband and wild-type mice, along with an outgroup (*P. maniculatus rufinus*), and the consensus sequence for 91 wild-caught individuals (Nebraska). R^2 is plotted for eight polymorphic sites [minor allele frequency (MAF) > 2%] in the Nebraska population (white vertical bars and bolded letters). Length heterozygosity resulted in some missing data; these sites were excluded from analysis. A derived amino acid deletion in exon 2 explains 13% of the phenotypic variation in Nebraska mice. (**B**) LD (left axis) and signature of selection (right axis) across the exon 2 flanking region. Position relative to exon 2 (top) or to the exon 2 serine deletion (bottom) is given. Each point is pairwise LD (|D'|, left axis) between a common polymorphism (MAF > 10%) and the serine deletion; black points are significant via χ^2 tests after Bonferroni correction. Also given is the CLR (right axis) as a function of position (solid line) for the wideband haplotype. The dotted line corresponds to the 95th percentile of the CLR (3.62); the arrow indicates the position that maximizes the ω statistic (ω_{max}). SFS- and LD-based analyses both point to the serine deletion as the putative target of selection.

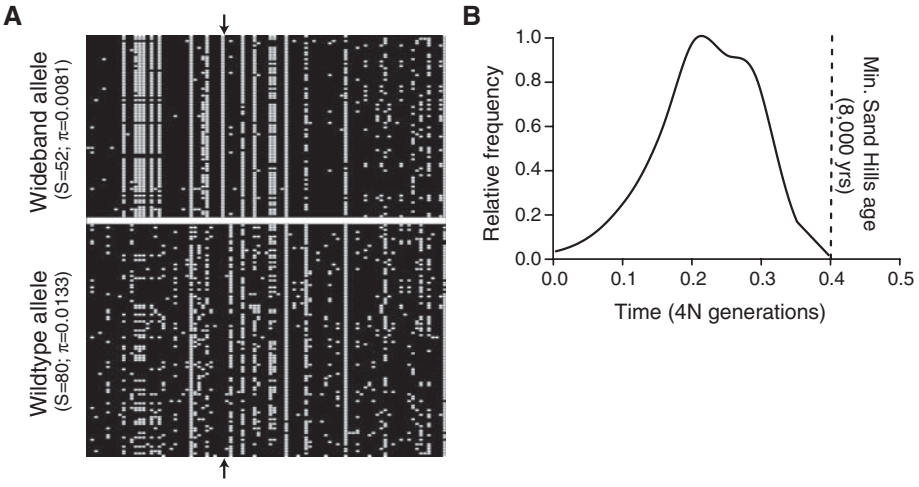

Fig. 4. The wideband mutation arose de novo after formation of the Sand Hills. (**A**) Variation in exon 2 flanking region for wideband ($a^{\Delta Ser}$, n = 80 alleles) and wild-type (a^{+}, n = 102 alleles) alleles. Rows are observed haplotypes; columns are variable nucleotide sites (black indicates ancestral, white indicates derived, and the outgroup is *P. maniculatus rufinus*). Arrows indicate the derived serine deletion. S and π are given for both haplotypes. Reduced variation among wideband alleles matches the pattern expected under selection on a de novo mutation. (**B**) Posterior probability distribution for the age (in 4N generations) of the beneficial wideband allele ($a^{\Delta Ser}$), and minimum age of the Sand Hills (8000 years, or 0.4 4N generations assuming N = 10,000 and 2 generations per year).

our 95% CI of s and calculation of ~2ln(2N)/s (*36*), we predict that the wideband allele should reach fixation (100% frequency) in 0.05 to 0.18 4N generations. These estimates were also similar to those obtained with a Bayesian approach (*37*), in which we found that over 99.9% of the posterior probability density falls on 0.5 ≥ T, ~85.4% on 0.25 ≥ T, and ~3.7% on 0.01 ≥ T, where T is the age of the beneficial allele in 4N generations (Fig. 4B). Given that the estimated age of the Sand Hills is 8000 to 10,000 years (or ~0.4 to 0.5 4N generations), our estimates suggest that this allele arose and underwent an incomplete sweep sometime after the formation of the Sand Hills.

Multiple lines of evidence suggest that the wideband allele arose de novo and was not a preexisting allele. First, the haplotype carrying the deletion has greatly reduced variation relative to the wild type (Fig. 4A), which is inconsistent with a model in which the causative mutation was neutrally segregating in the population before any selective pressure (*38*). Second, the U-shaped SFS is most consistent with a model in which selection acts on a newly arising mutation (fig. S3). If the beneficial mutation existed on multiple haplotypes before the selective pressure, we would expect to see an excess of intermediate frequency mutations, which was not observed (*38*). Finally, the posterior probability density of the allele age falls entirely within the estimated age of the Sand Hills (Fig. 4B).

Taken together, our results demonstrate that variation at the *Agouti* locus is responsible for adaptive coloration in deer mice living on the Nebraska Sand Hills. Although it is clear that a derived increase in *Agouti* expression leads to wider hair bands and lighter camouflaging color, whether and by which mechanism an amino acid deletion ($a^{\Delta Ser}$) leads to a change in gene expression and ultimately phenotypic evolution is still unknown. From our estimates of the strength and timing of selection acting on this adaptive allele, we conclude that the wideband *Agouti* allele arose de novo after the colonization of a novel selective environment, which is counter to recent studies demonstrating adaptation arising from standing genetic variation (*39*–*41*). This suggests that rapid adaptive change—such as the recent evolution of cryptic coloration in Sand Hill mice—need not always rely on preexisting genetic variation.

References and Notes

1. D. T. Lewis, in *An Atlas of the Sand Hills*, A. Bleed, C. Flowerday, Eds. (Conservation and Survey Division, Univ. Nebraska-Lincoln, Lincoln, 1989), p. 57.
2. T. S. Ahlbrandt, S. G. Fryberger, in *Recent and Ancient Nonmarine Depositional Environments*, F. G. Ethridge, R. M. Flores, Eds. (Society of Economic Paleontologists and Mineralogists, Tulsa, OK, 1981), pp. 293–314.
3. L. R. Dice, *Contrib. Lab. Vertebrate Genet. Univ. Michigan* **15**, 1 (1941).
4. L. R. Dice, *Contrib. Lab. Vertebrate Biol. Univ. Michigan* **34**, 1 (1947).
5. H. E. Hoekstra, K. E. Drumm, M. W. Nachman, *Evolution* **58**, 1329 (2004).
6. J. B. Swinehart, in *An Atlas of the Sand Hills*, A. Bleed, C. Flowerday, Eds. (Conservation and Survey Division, Univ. Nebraska-Lincoln, Lincoln, 1989), pp. 43–56.
7. D. B. Loope, J. Swinehart, *Gt. Plains Res.* **10**, 5 (2000).
8. I. J. Jackson, *Annu. Rev. Genet.* **28**, 189 (1994).
9. H. E. Hoekstra, *Heredity* **97**, 222 (2006).
10. W. B. McIntosh, *Contrib. Lab. Vertebrate Biol. Univ. Michigan* **73**, 1 (1956).
11. Materials and methods are available as supporting material on *Science* Online.
12. S. J. Bultman, E. J. Michaud, R. P. Woychik, *Cell* **71**, 1195 (1992).
13. R. J. Miltenberger *et al.*, *Genetics* **160**, 659 (2002).
14. M. Miller *et al.*, *Genes Dev.* **7**, 454 (1993).
15. H. Vrieling, D. Duhl, S. Millar, K. Miller, G. Barsh, *Proc. Natl. Acad. Sci. U.S.A.* **91**, 5667 (1994).
16. B. E. Horner, G. L. Potter, S. Van Ooteghem, *J. Hered.* **71**, 49 (1980).
17. E. P. Kingsley, C. D. Wiley, H. E. Hoekstra, *PLoS One* **4**, e6435 (2009).
18. K. M. Dodson, thesis, University of South Carolina, Columbia (1982).
19. P. J. Wittkopp, B. K. Haerum, A. G. Clark, *Nature* **430**, 85 (2004).
20. S. Bultman *et al.*, *Genes Dev.* **8**, 481 (1994).
21. J. K. Pritchard, M. Stephens, P. Donnelly, *Genetics* **155**, 945 (2000).
22. D. Falush, M. Stephens, J. K. Pritchard, *Genetics* **164**, 1567 (2003).
23. P. Jackson *et al.*, *Chem. Biol.* **13**, 1297 (2006).
24. J. Storz *et al.*, *PLoS Genet.* **3**, e45 (2007).
25. A. P. McGregor *et al.*, *Nature* **448**, 587 (2007).
26. Y. Kim, W. Stephan, *Genetics* **160**, 765 (2002).
27. C. Meiklejohn, Y. Kim, D. Hartl, J. Parsch, *Genetics* **168**, 265 (2004).
28. J. Jensen, Y. Kim, V. DuMont, C. Aquadro, C. Bustamante, *Genetics* **170**, 1401 (2005).
29. Y. Kim, R. Nielsen, *Genetics* **167**, 1513 (2004).
30. J. Jensen, K. Thornton, C. Bustamante, C. Aquadro, *Genetics* **176**, 2371 (2007).
31. C. Laurie *et al.*, *PLoS Genet.* **3**, e144 (2007).
32. J. Jensen, K. Thornton, C. Aquadro, *Mol. Biol. Evol.* **25**, 438 (2008).
33. L. M. Mullen, H. E. Hoekstra, *Evolution* **62**, 1555 (2008).
34. E. Creed, *Proc. R. Soc. London B. Biol. Sci.* **190**, 135 (1975).
35. B. Clarke, J. Murray, *Heredity* **17**, 445 (1962).
36. W. Stephan, T. Wiehe, M. Lenz, *Theor. Popul. Biol.* **41**, 237 (1992).
37. M. Przeworski, *Genetics* **164**, 1667 (2003).
38. M. Przeworski, G. Coop, J. Wall, *Evolution* **59**, 2312 (2005).
39. J. L. Feder *et al.*, *Proc. Natl. Acad. Sci. U.S.A.* **100**, 10314 (2003).
40. P. Colosimo *et al.*, *Science* **307**, 1928 (2005).
41. R. Barrett, D. Schluter, *Trends Ecol. Evol.* **23**, 38 (2008).

42. We thank J. Crossland and M. Dewey for assistance with crosses; W. Dawson for his advice; M. Chin, B. Hehli, and K. Hogan for laboratory assistance; J. Chupasko, E. Kay, M. Manceau, and J. Weber for field assistance; J. Demboski and the Denver Museum of Nature and Science for logistical support; J. Losos and B. Payseur for comments; and G. Barsh for ongoing discussion about *Agouti*. C.R.L. was supported by a Ruth Kirschstein National Research Service Award from NIH; J.D.J. was supported by a NSF Biological Informatics Postdoctoral Fellowship. Laboratory and fieldwork was funded by NSF and the Museum of Comparative Zoology at Harvard University. *P. maniculatus* were collected under the Nebraska Game and Parks Commission Scientific and Educational Permit 901, and voucher specimens were deposited in the Mammal Department at the Museum of Comparative Zoology. Sequence data were deposited in GenBank (accession numbers GQ337976 to GQ337987 and GQ340804 to GQ340896).

Supporting Online Material

www.sciencemag.org/cgi/content/full/325/5944/1095/DC1
Materials and Methods
Figs. S1 to S3
Tables S1 to S5
References

4 May 2009; accepted 8 July 2009
10.1126/science.1175826